npj | Climate and Atmospheric Science

www.nature.com/npjclimatsci

ARTICLE OPEN

Check for updates

Anthropogenic warming and intraseasonal summer monsoon variability amplify the risk of future flash droughts in India

Vimal Mishra[1,2]✉, Saran Aadhar[1] and Shanti Shwarup Mahto[2]

Flash droughts cause rapid depletion in root-zone soil moisture and severely affect crop health and irrigation water demands. However, their occurrence and impacts in the current and future climate in India remain unknown. Here we use observations and model simulations from the large ensemble of Community Earth System Model to quantify the risk of flash droughts in India. Root-zone soil moisture simulations conducted using Variable Infiltration Capacity model show that flash droughts predominantly occur during the summer monsoon season (June–September) and driven by the intraseasonal variability of monsoon rainfall. Positive temperature anomalies during the monsoon break rapidly deplete soil moisture, which is further exacerbated by the land-atmospheric feedback. The worst flash drought in the observed (1951–2016) climate occurred in 1979, affecting more than 40% of the country. The frequency of concurrent hot and dry extremes is projected to rise by about five-fold, causing approximately seven-fold increase in flash droughts like 1979 by the end of the 21st century. The increased risk of flash droughts in the future is attributed to intraseasonal variability of the summer monsoon rainfall and anthropogenic warming, which can have deleterious implications for crop production, irrigation demands, and groundwater abstraction in India.

npj Climate and Atmospheric Science (2021)4:1 ; https://doi.org/10.1038/s41612-020-00158-3

INTRODUCTION

A large fraction of 1.4 billion people in India depends on agriculture for their livelihood. Agriculture contributes considerably to the Indian gross domestic product (GDP)[1]. Weather and climate extremes hamper food production, farm-income, and overall well-being of the people living in India[2–6]. India experiences droughts that can lead to a prolonged period of water scarcity[7,8]. Droughts pose deleterious impacts on natural resources, crop production, and environment[1,8–10]. Since the summer monsoon rainfall is the primary source of surface water availability in the large part of the country, the onset of droughts in India is well associated with the failure of the summer monsoon[1,11]. Year-to-year variability of the summer monsoon precipitation in India is linked with the large-scale atmospheric and oceanic forcing[7,12,13]. Positive sea surface temperature (SST) anomalies over the central Pacific Ocean (El Nino) often result in weaker summer monsoon leading to meteorological droughts in India[1,9,14]. Persistent meteorological droughts translate to agricultural and hydrological droughts, which cause devastating impacts on food production and water availability in the country[15–17].

Causes and consequences of droughts caused by the failure of the summer monsoon in India are well studied[1,12,18–20]. However, drivers and impacts of flash droughts[21,22] in India are not examined. Flash droughts occur due to the rapid depletion of soil moisture caused either by precipitation deficit or increased air temperature or both[21–25]. Favourable crop growing conditions can translate to extreme dry conditions within a few days to weeks due to flash droughts[22,26]. Therefore, flash droughts in the crop growing season adversely affect agriculture and ecosystem leading to considerable economic losses[26–28]. Understanding of flash droughts in India is vital as agricultural activities heavily rely on the summer monsoon and groundwater based irrigation[9,29]. Thus, the increased frequency of flash droughts during the crop growing season can result in increased irrigation demands. Increased irrigation demands in a large area in short-time can lead to increased groundwater pumping from the already depleting aquifers in India[29,30].

India is projected to witness extreme climatic conditions in the future[9,31–35]. Extreme hot and dry conditions that lead to flash droughts can occur more frequently under climate change[32]. However, increased risk of flash droughts under a warming climate is less recognized[22,36,37] in comparison to conventional droughts[38–42]. Given the significant rise in the warming that is projected in the future in India[31,32,43,44], the risk of flash droughts in the future in India seems unavoidable. However, the changes in the frequency and characteristics of flash droughts in India are not examined. Here, we use observations and large ensemble simulations from the Community Earth System Model (CESM-LENS) to reconstruct root-zone soil moisture for the observed (1951–2016) and future climate. The root-zone soil moisture was used to examine the role of anthropogenic warming on the projected changes in the frequency of flash droughts in India.

RESULTS

Flash droughts in the observed climate, 1951–2016

First, we identify the major flash droughts that occurred during the observed climate (1951–2016) in India. We used the VIC model simulated soil moisture using the observed meteorological forcing from the India meteorological department (IMD[45,46]). The VIC model estimates evapotranspiration using Penman–Monteith method, which avoids uncertainty that can arise due to estimation of evaporative demands based on just temperature[47,48]. Due to the lack of long-term root-zone soil moisture observations, soil moisture simulated using the land surface models has been widely used for the drought assessment[17,18,49,50]. The performance of the VIC simulated hydrologic variables was carefully evaluated against in-situ and satellite-based observations in the previous studies[17,51]. The VIC model simulations were successfully evaluated against observed streamflow, evapotranspiration (ET), and soil

[1]Civil Engineering, Indian Institute of Technology (IIT), Gandhinagar, India. [2]Earth Sciences, Indian Institute of Technology (IIT), Gandhinagar, India. ✉email: vmishra@iitgn.ac.in

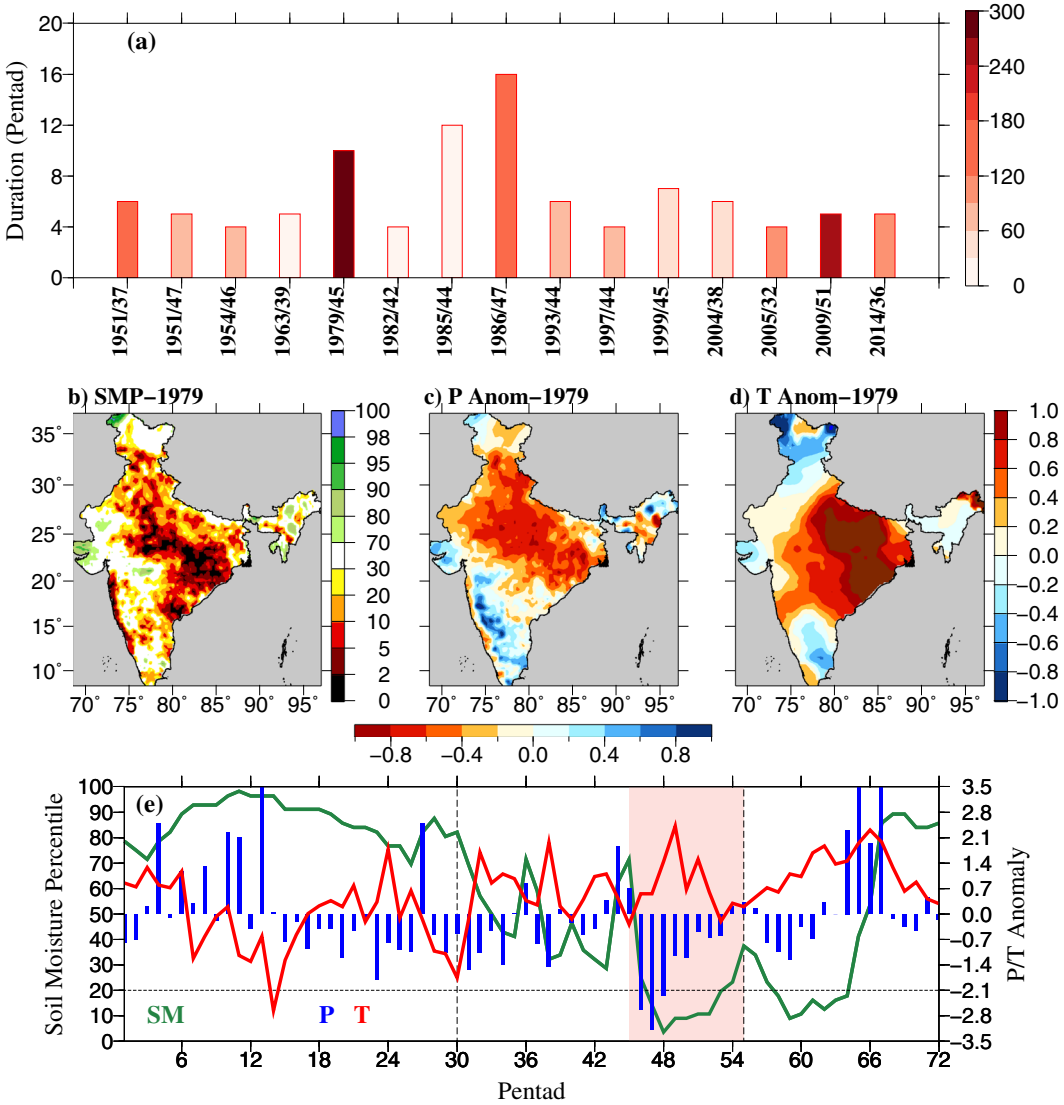

Fig. 1 Flash droughts in the observed climate in India during 1951–2016. a Duration and overall severity score (color scale) of flash droughts in India, **b** Soil moisture percentile of 1979 flash drought during its peak intensity, **c** mean precipitation anomaly during the 1979 flash drought, **d** mean temperature anomaly during 1979 flash drought, and **e** evolution of the 1979 flash drought in India shown using soil moisture percentile and precipitation/temperature anomalies. Shaded pink region in **e** shows the duration of the 1979 flash drought. Vertical dotted black lines in **e** show the summer monsoon season (30th to 55th pentad).

moisture[17,51]. Also, the VIC model-simulated soil moisture was compared against soil moisture from Global Land Evaporation Amsterdam Model (GLEAM[52]) and soil moisture from ERA-5 (Supplementary Fig. 1). The VIC simulated soil moisture anomalies compare well against the GLEAM and ERA-5 products (Supplementary Fig. 1), which further provides us with the confidence to use the VIC model-simulated soil moisture for the flash drought assessment in India.

Flash droughts (Supplementary Fig. 2, see methods for details) were identified using the all-India averaged VIC model-simulated soil moisture for the observed period of 1951–2016 (Fig. 1a). All 15 flash droughts occurred during the summer monsoon season (Fig. 1a, Supplementary Table 1). Flash drought characteristics including duration (in pentad—5-day period), intensity, and areal extent were estimated for India and overall severity score (duration × intensity × areal extent)[16] was used to rank flash droughts. The overall severity score combines the three characteristics of flash drought and provides indirect information on the impacts[16]. We assume that a widespread, longer-lasting, and intense flash drought can cause harmful consequences for crop production. The top five flash droughts based on the overall severity score occurred in 1951, 1979, 1986, 2005, and 2009 (Supplementary Table 1). The 1979 flash drought had the highest overall severity score (Supplementary Table 1). The second-ranked flash drought occurred in 2009 (Supplementary Table 1). The duration estimated using all-India averaged soil moisture percentile for 1979, and 2009 flash droughts were 10 and 5 pentads, respectively (Fig. 1a, Supplementary Table 1). The 1979 flash drought affected more than 40% of the country, while about 28% of India was influenced by the 2009 flash drought (Fig. 1). The longest-lasting flash drought occurred in 1986 with a duration of 16 pentads. Out of 15 flash droughts, ten occurred after 1980. Moreover, the flash droughts of 2005 and 2009 had the warmest mean temperature anomalies (Supplementary Table 1). Overall, there has been an increase in the frequency of flash droughts in the post-1980 period in India. Also, the 1979 flash drought of the monsoon season was the worst event that the country experienced during the entire record of 1951–2016 (Fig. 1).

As the 1979 flash drought was the worst event that India faced during 1951–2016, we further diagnosed the spatial and temporal

patterns associated with precipitation, air temperature, and soil moisture (Fig. 1b–e). During the peak intensity (48th pentad, Supplementary Table 1), soil moisture percentiles were significantly low in the Indo-Gangetic Plain, eastern parts, and Western Ghats of India (Fig. 1b). Thus, the 1979 flash drought was not localized; rather it covered a large part (~40%) of the country. More importantly, the Indo-Gangetic Plain was significantly affected by the flash drought of 1979. Standardized precipitation anomalies averaged over the entire duration (10 pentads) of the 1979 flash drought showed that a large part of the north and central India experienced lower than normal precipitation, which triggered the flash drought. A strong warm temperature anomaly that caused high evaporative demand was present in the large part over the Indo-Gangetic Plain and eastern India (Fig. 1d). The 1979 flash drought occurred between 45 and 55th pentad, which is part of the monsoon season (30–55 pentad) (Fig. 1e). The flash drought was caused by the dry period that started around 45th pentad. The peak intensity of flash drought based on soil moisture percentile occurred three pentads later (i.e. 48th pentad). Precipitation break and depleted soil moisture exacerbated the warm temperature anomalies due to increased evaporative demands (Fig. 1e). Therefore, the positive temperature anomaly of more than 2 °C was caused by the monsoon break and land-atmosphere feedback[53,54].

Drivers of flash droughts in India

Atmospheric conditions [geopotential height at 500hPa, mean sea level pressure, wind at 850 hPa, and integrated water vapour (IWV)] were analyzed for the flash drought of 1979 (Supplementary Fig. 3). Atmospheric anomalies for one pentad before the onset, during peak intensity, and one pentad after the termination of the flash drought were analyzed (Supplementary Fig. 3). Negative geopotential height anomaly was centred over India before the onset of the 1979 flash drought. A large part of the country experienced positive geopotential height anomaly during the peak of the 1979 flash drought. Negative geopotential height anomaly was observed after the termination of the flash drought. Similarly, mean sea level pressure and lower tropospheric wind anomalies indicate favourable conditions of an active phase of the summer monsoon[53,55] before the onset of the 1979 flash drought. A strong flow of moisture carrying westerly winds from the Indian Ocean and low pressure over India resulted in positive rainfall anomalies before the onset of the flash drought (Fig. 1e, Supplementary Fig. 3). However, during the peak of the flash drought, positive mean sea level pressure and weak moisture carrying wind flow exhibit the condition that resembles the monsoon break[53,55,56] (Fig. 1e). After the termination of the 1979 flash drought, the negative sea level pressure and westerly wind flow over the Indo-Gangetic Plain were present (Supplementary Fig. 3). Since the termination of the flash drought overlaps with the end of the monsoon season, strong westerly wind flow from ocean to land was not seen after the termination of the flash drought (Supplementary Fig. 3). Similar conditions that favoured rainfall before the onset, during the peak, and after the termination of the 1979 flash drought were noticed from the integrated water vapour anomalies (Supplementary Fig. 3). Overall, geopotential height, mean sea level pressure, wind, and integrated water vapour anomalies indicate the atmospheric drivers of the worst flash drought that occurred during 1979–2016 period in India exhibit the patterns similar to those occurring during the monsoon break.

We constructed composite of geopotential height (at 500hPa), mean sea level pressure, wind (at 850 hPa), and integrated water vapour anomalies for all the flash droughts that occurred during 1979–2016 to examine the role of atmospheric anomalies during the flash droughts in India (Fig. 2, Supplementary Figs 4,5). Out of 15, four flash droughts that occurred before 1979 (1951, 1954, and 1963) were excluded from the composite analysis as ERA-5 reanalysis is available only after 1979. Positive geopotential height, high mean sea level pressure, weaker lower tropospheric winds, and negative integrated water vapour anomalies occur during the peak of the flash droughts (Fig. 2a–c, Supplementary Figs 4,5). Long monsoon breaks cause a rise in air temperature[56], which can further exacerbate soil moisture depletion[54,57]. We derived the composites of atmospheric variables for all the concurrent extreme hot (temperature anomaly more than one standard deviation) and dry (soil moisture anomaly less than −1 standard deviation) pentads in the monsoon season during 1979–2016. We did so to confirm if the atmospheric conditions during the flash droughts are associated with the low soil moisture and high temperature (Fig. 2d–f). Atmospheric conditions during the concurrent extreme hot and dry pentads are similar to those obtained during the peak flash droughts. Thus, the flash droughts during the monsoon season are triggered by the monsoon breaks and amplified by the land-atmospheric interaction leading to extreme hot and dry conditions. Moreover, composites obtained for the peak flash droughts and extreme hot and dry conditions are consistent with the monsoon breaks[53,55,56].

The monsoon breaks are associated with the weakening of lower tropospheric moisture carrying westerly winds, which in turn result in a deficit in integrated water vapour flux over land[58]. In contrast, concurrent extreme wet (soil moisture anomaly above one std) and cool (temperature anomaly below one std) anomaly pentads show atmospheric signatures that resemble the active phase of the summer monsoon[53,59–61]. For instance, negative geopotential height and mean sea level pressure anomalies give rise to strong monsoonal flow that increases moisture carrying clouds over the land during the active phase of the summer monsoon (Fig. 2g–i). Overall, breaks during the summer monsoon can cause concurrent extreme hot and dry conditions that rapidly deplete soil moisture leading to flash droughts in India. Also, the frequency of extreme hot pentads has increased during 1951–2016, which is likely to increase in the future, causing more favourable conditions for flash droughts under the warming climate (Supplementary Fig. 6).

Flash droughts in the future climate

Next, we examined if the concurrent extreme dry and hot conditions that cause flash droughts during the monsoon will occur more frequently in a warming climate. We used a large ensemble from the fully coupled Community Earth System Model (CESM-LENS[62]). The CESM-LENS simulations are available from 40 ensemble members, which capture the summer monsoon precipitation variability and its coupling with sea surface temperature (SST) reasonably well[9]. In contrast to most global climate models from the Coupled Model Intercomparison Project −5 (CMIP-5)[63,64], CESM-LENS reproduces coupled variability between the number of rainy days (days with precipitation more than 1 mm) and SST reasonably well during the summer monsoon season (Supplementary Fig. 7). For instance, the role of El Nino Southern Oscillation (ENSO) and Indian Ocean Dipole (IOD) on the number of rainy days during the monsoon is well captured in the first mode of coupled variability identified using Maximum Covariance Analysis (MCA[9,65]). CESM-LENS simulations effectively capture the seasonal cycle of precipitation and air temperature over India (Supplementary Fig. 8). Since daily root-zone soil moisture simulations are not available directly from CESM-LENS, the VIC model was used to simulate soil moisture for each CESM-LENS ensemble member for 1920–2100 period. As expected, there is a bias between root-zone soil moisture from the CESM-LENS and observed forcing from the IMD, which can be attributed to cool bias in air temperature in the CESM-LENS (Supplementary Fig. 8). Nonetheless, the bias does not have a significant influence in the estimation of concurrent extreme hot, and dry pentads as the

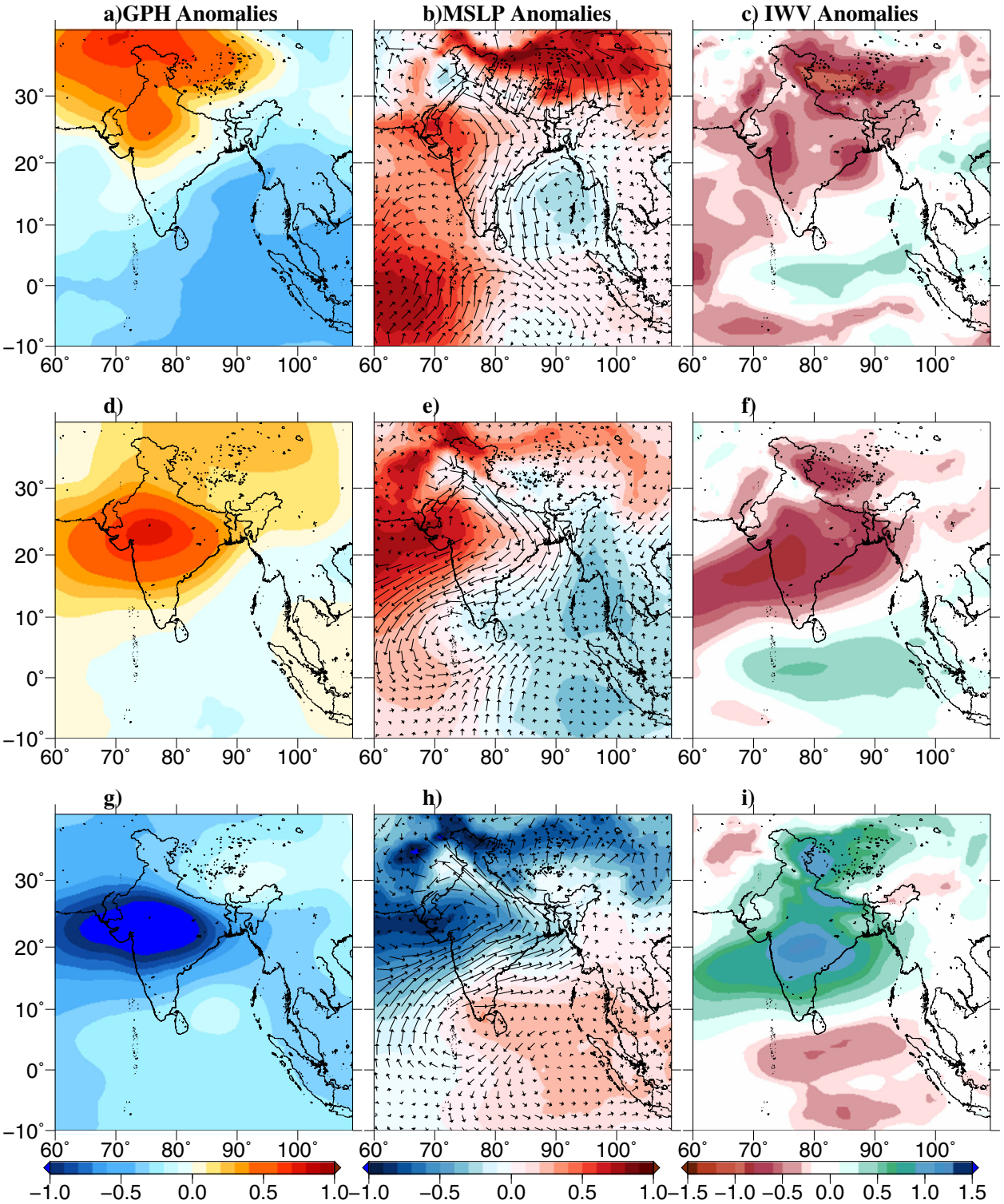

Fig. 2 Atmospheric anomalies composites for peak flash droughts during 1979–2016. a–c Anomaly composites of geopotential height (m), mean sea level pressure (hPa), and integrated water vapor (kg/m/s) during the peak of flash droughts that occurred in India during 1979–2016, **d–f** same as **a–c** but for all extreme dry and hot pentads during 1979–2016, and **g–i** same as **a–c** but for all extreme wet and cool pentads during 1979–2016. Extreme dry and hot pentads were identified with soil moisture anomaly less than −1 standard deviation and temperature anomaly more than +1 standard deviation. Pentad anomalies for each atmospheric variables were estimated using ERA-5 reanalysis data.

standardized soil moisture and air temperature anomalies were estimated against the historical period of each CESM-LENS ensemble member.

The frequency of extreme hot, dry, and concurrent hot and dry pentads were estimated using the CESM-LENS simulations for 1951–2100 period (Fig. 3). A 30-year moving window analysis shows a considerable rise in the frequency of extreme dry and extreme hot pentads under the warming climate (Fig. 3). The frequency of extreme dry pentads is projected to rise by a factor of 2.5 (from the current period) by the end of the 21st century

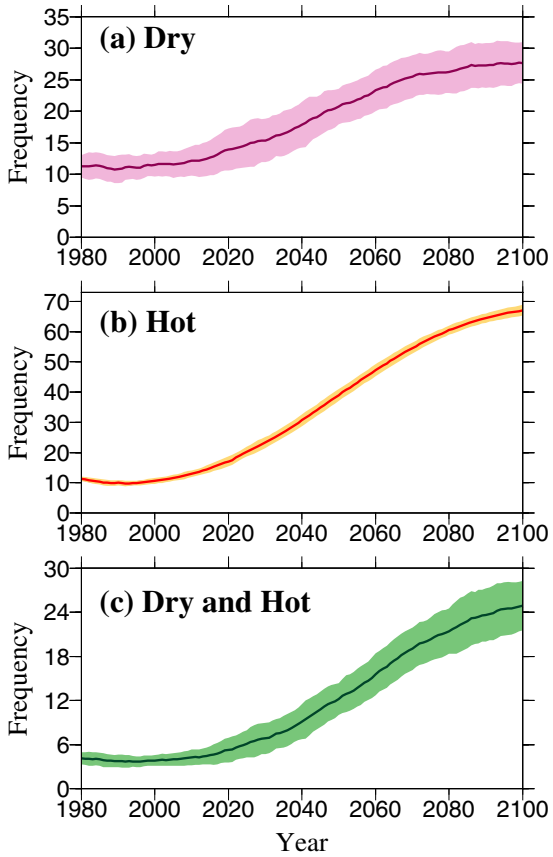

Fig. 3 Projected changes in the frequency (per year) of extreme dry, hot, and dry and hot pentads from CESM-LENS ensemble during 1951–2100. a 30-year moving mean frequency (per year) of extreme dry soil moisture pentads, **b** 30-year moving mean frequency (per year) of extreme hot pentads, and **c** 30-year moving mean frequency (per year) extreme dry and hot pentads. Extreme dry and hot pentads were estimated based on the standardized departure more than one standard deviation from the reference period of 1971–2000. Shaded area shows uncertainty due to internal climate variability in 40 CESM-LENS ensemble members.

(Fig. 3a). More importantly, the frequency of extreme hot pentads is projected to increase by a factor of six by the end of the 21st century based on CESM-LENS simulations under the RCP 8.5 (Fig. 3b). The significant increase in extreme dry and extreme hot pentads is likely to result in a four-times rise in concurrent extreme warm and dry pentads from the current level under the future climate. Increase in concurrent extreme hot and dry pentads can trigger more flash droughts in the future, which may get amplified due to land-atmospheric interaction under the warming climate[66,67].

We estimated changes in the frequency of flash droughts like 1979 in the observed climate in the future. India experienced the worst flash drought in 1979, which affected agriculture and water availability in a large part of the country[68]. The flash drought lasted about ten pentads, affected more than 40% of the country, mean intensity was less than −1, and overall severity score reached around 300. The frequency of flash droughts that crossed the benchmark characteristics of the 1979 flash drought was estimated using the CESM-LENS simulations (Fig. 4). More than 1200 years (30-year period from each of the 40 ensemble members) simulations from CESM-LENS show that the frequency of flash droughts with a duration of more than ten pentads is projected to increase about six-fold by the end of 21st century (Fig. 4a). Similarly, the frequency of flash droughts covering more than 40% of the country is likely to rise approximately eight-fold

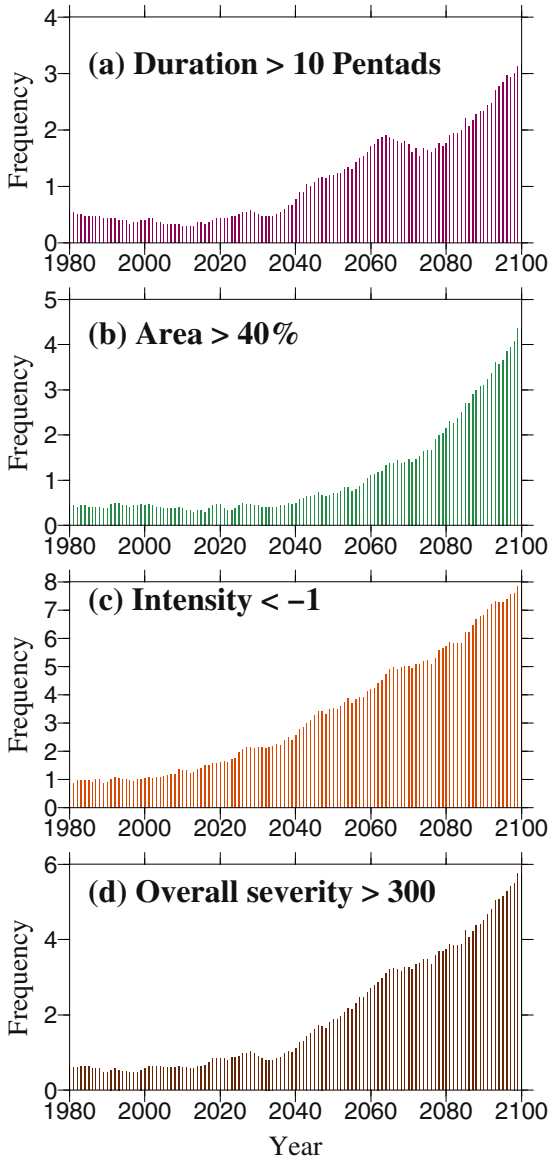

Fig. 4 Flash drought projections in India under the projected future climate using CESM-LENS ensemble. a 30-year moving mean frequency of flash drought with duration more than 10 pentads during 1951–2100, **b** same as **a** but for the flash drought that had areal extent more than 40%, **c** same as a but for the flash drought that had mean intensity less than −1, and **d** same as **a** but for the flash droughts that had overall severity score more than 300.

by the end of the 21st century (Fig. 4b). Moreover, the frequency of flash droughts with mean intensity −1 or less is projected to increase by 7-fold under the RCP 8.5 by the end of 21st century (Fig. 4c). Combining all together, India may witness an increase of about 7–8-fold rise in the frequency of flash droughts (like 1979) by the end of the 21st century (Fig. 4d). Overall, the VIC model-simulated soil moisture using CESM-LENS forcing show a considerable rise in the concurrent extreme hot and dry pentads and flash droughts under the projected future climate in India.

Causes of the projected increase in flash droughts in India

The frequency of flash droughts is projected to rise in the future under warming climate despite the expected increase in the summer monsoon precipitation[64,69]. The monsoon season precipitation is projected to rise by 8–10% under the future climate

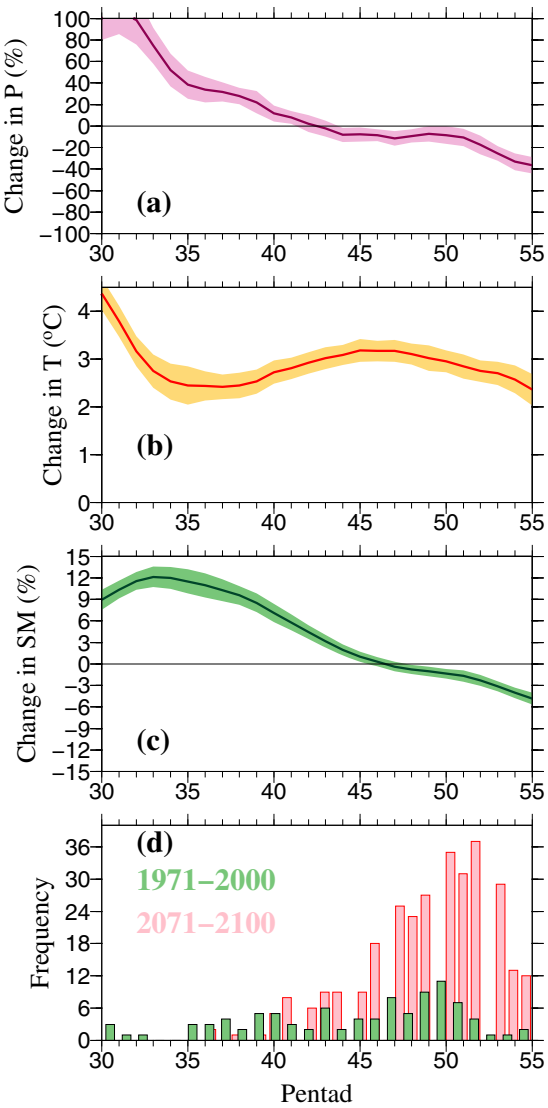

Fig. 5 Projections of precipitation, air temperature, soil moisture, and frequency of flash droughts during the monsoon season from CESM-LENS ensemble. **a** projected change in precipitation (%) for the pentads during the monsoon season, **b** same as **a** but for air temperature, **c** same as **a** but for soil moisture. Projected changes in the end of 21st century (2071–2100) was estimated against the reference period of 1971–2000. Shaded area in **a**–**c** shows the uncertainty (estimated using one standard deviation) based on the 40 ensemble members from CESM-LENS. **d** The frequency of flash droughts that occurred during the monsoon season for 1971–2000 and 2071–2100 periods.

based on the CESM-LENS simulations[9] (Supplementary Fig. 9). The projected rise in the summer monsoon precipitation results in an increase of 3–4% in the monsoon season root-zone soil moisture indicating an overall warmer and wetter climate from the agricultural activities perspective in the future (Supplementary Fig. 9). If the monsoon season precipitation is projected to rise, then what causes an increase in the hot and dry extreme and more frequent severe flash droughts in the future? To address this question, we examined the intraseasonal variability in the projected changes in precipitation, air temperature, and soil moisture during the monsoon season (Fig. 5). The projected change in precipitation, air temperature, and soil moisture was estimated for each pentad during the monsoon season against the reference period of 1971–2000 using simulations from 40 ensemble members of CESM-LENS (Fig. 5). CESM-LENS simulations project a considerable increase in precipitation during the early monsoon (30–42 pentads) in the future climate. However, precipitation is projected to decline during the late monsoon season (43–55 pentad). The higher projected increase in the early summer monsoon precipitation contributes to the projected rise in the seasonal mean, indicating wetter conditions in the future (Supplementary Fig. 9). While the projected decline in precipitation during the late monsoon is not as high as the increase in the early monsoon, it has implications for the response of soil moisture with the changes in precipitation and temperature. Air temperature is projected to rise by 2–3 °C in all the pentads during the monsoon season (Fig. 5). The decline in precipitation combined with the projected warming during the late monsoon season results in 3–4% decrease in root-zone soil moisture (Fig. 5c). Therefore, intraseasonal variability in precipitation along with the significant warming gives rise to the frequency of flash droughts during the late monsoon season under the warming climate in India (Fig. 5d). The intraseasonal variability in summer monsoon precipitation can be different in different global climate models (GCMs). Notwithstanding our findings are based on a single (CESM) GCM, the intraseasonal variability in summer monsoon rainfall combined with increased air temperature under the future climate can have a considerable influence on the occurrence of flash droughts in India.

Role of anthropogenic warming

Concurrent hot and dry events and intraseasonal variability in the monsoon season cause flash droughts in India. A majority of flash droughts in the observed and future climate occur during the monsoon season. We examined the role of greenhouse gas emissions (GHG), industrial aerosols (AER), and land-use/land-cover change (LULC) using the CESM simulations conducted under the single-forcing experiment[70] (see methods for more details). In the single-forcing experiments, the effect of GHG, AER, and LULC was kept the same as of 1920. Therefore, the influence of XGHG (no GHG), XAER (no industrial aerosols), and XLULC (no land-use/land-cover change) can be estimated by comparing to the CESM-LENS simulations based on the all (ALL: natural + anthropogenic) forcing. We estimated concurrent extreme hot and dry events in XGHG, XAER, XLULC, and compared with the same ensemble members under the ALL scenario from the CESM-LENS (Fig. 6). Anthropogenic GHG emissions have a significant influence on the frequency of concurrent extreme hot and dry events (Fig. 6a). For instance, the frequency of concurrent extreme hot and dry events that cause flash droughts under the ALL scenario is significantly higher than XGHG under the historical and projected future climate (Fig. 6a). The risk ratio (ratio of the frequency of concurrent hot and dry events in the ALL and the XGHG) of concurrent extreme hot and dry events during the monsoon season projected to be about 16–18 by the end of the 21st century (Fig. 6d). Removal of industrial aerosols results in the rise of concurrent extreme hot and dry events during the monsoon season in India. Removal of industrial aerosols causes an increase in solar radiation that can elevate air temperature[70]. However, the risk ratio (ALL/XAER) remains less than one in both historical and projected climate (Fig. 6b, e). The influence of LULC on the frequency of concurrent hot and dry extremes during the monsoon season in India was substantially lesser than that of GHG. Our soil moisture simulations only account for the changes in meteorological forcing (from CESM) caused by the LULC, which do not reflect the influence of LULC changes on hydrological processes through the land surface model (Fig. 6c, f). Overall, anthropogenic warming caused by GHG emissions is directly linked with the occurrence of concurrent extreme hot and dry events during the monsoon that causes flash droughts in India. In addition to anthropogenic warming, the intraseasonal variability in the monsoon season

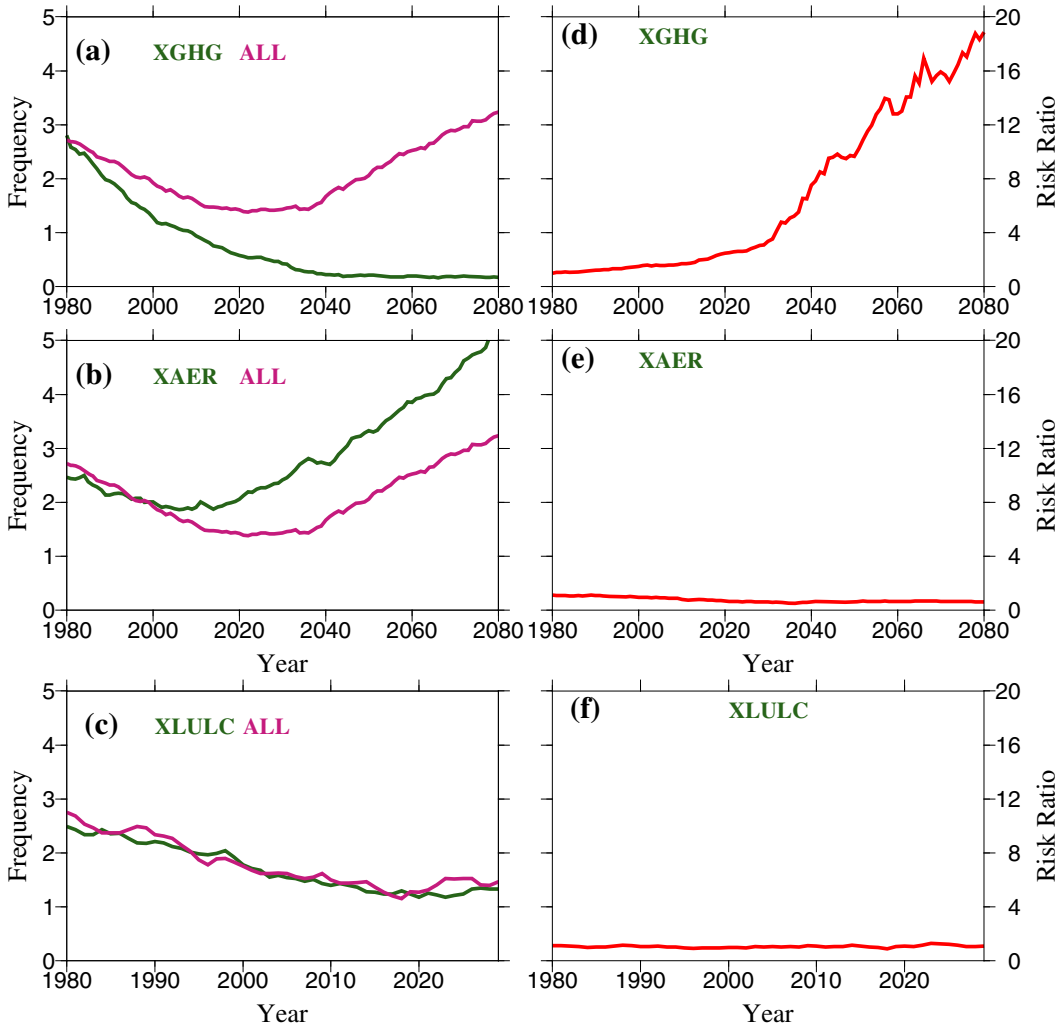

Fig. 6 The influence of greenhouse gas emissions (GHG), industrial aerosols (AER), and land-use/land-cover (LULC) on concurrent hot and dry extremes during the summer monsoon season in India. a–c The frequency (per year) of concurrent hot and dry extremes under no greenhouse gas emission (XGHG), no industrial aerosols (XAER), and no land-use/land-cover change (XLULC) and under ALL (natural + anthropogenic forcing) scenarios for 1951–2080, 1951–2080, and 1951–2029 periods, respectively. **d–f** Risk ratio (frequency in the ALL/frequency in XGHG/XAER/XLULC) estimated for XGHG, XAER, and XLULC and ALL scenarios. The effect of GHG, AER, and LULC was estimated using the single-forcing experiments from CESM for 20, 20, and 5 ensemble members, respectively.

precipitation also plays a vital role in the occurrence of flash droughts.

DISCUSSION

Monsoon breaks and positive temperature anomalies caused the observed flash droughts. Atmospheric conditions during flash droughts resemble monsoon breaks with positive geopotential and mean sea level pressure anomalies over land, causing weakened westerly flow from the Indian Ocean. Among the fifteen flash droughts identified in India during the observed record of 1951–2016, the 1979 drought was the worst, which affected about 40% of the entire country. The risk of concurrent extreme hot and dry pentads and flash droughts was quantified using the simulations from 40 ensemble members of CESM-LENS. The frequency of concurrent extreme hot and dry pentads is projected to rise considerably under the warming climate over India. This increase in the frequency of concurrent hot and dry extremes is projected to cause ~7–8 fold rise in the frequency of flash droughts like the year 1979 flash drought in the observed climate in India. The projected rise in the frequency of flash droughts in India during the monsoon season is associated with the intraseasonal variability in the monsoon season precipitation and anthropogenic warming. Notwithstanding the projected rise in the monsoon season precipitation in the future, the projected increase in flash droughts during the monsoon season is largely due to warming and decline in soil moisture in the late monsoon season. The role of GHG, AER, and LULC was examined using the simulations from the single-forcing experiment of CESM-LENS. The anthropogenic warming caused by greenhouse gas emissions has significantly increased the risk of concurrent hot and dry extremes that cause flash droughts in the monsoon season in India. Increased risk of flash droughts and concurrent hot and dry extremes in the future will have implications for agriculture and water availability. Widespread flash droughts and elevated temperature during the crop growing seasons can increase the irrigation demands indirectly impacting the depleting groundwater resources in the country.

METHODS

Observed and projected climate data

We obtained gridded daily precipitation available at 0.25° from the India Meteorology Department (IMD) for 1951–2016 period. The gridded

precipitation data are based on more than 6500 rainfall observation stations located across India[45]. The gridded rainfall data captures the large-scale variability in the Indian summer monsoon and orographic features of rainfall in the foothills of Himalaya and Western Ghats[45]. The gridded precipitation data has been widely used for drought assessment in India[17,71]. Similar to gridded precipitation, gridded daily maximum and minimum temperatures were also obtained from IMD. Gridded temperature data is based on more than 350 observation stations located across India[46]. The dataset is available at 1° spatial and daily temporal resolution, which was regridded to 0.25° using a Synergraphic Mapping algorithm that considers the digital elevation model and lapse rate[72].

We obtained daily precipitation, maximum and minimum temperatures, and wind speed from the Community Earth System Model (CESM)-Large Ensemble (LENS) project (http://www.cesm.ucar.edu/projects/community-projects/LENS/)[62]. CESM-LENS provides fully coupled simulations at 1° spatial resolution for 40 ensemble members for 1920–2100 period. Each ensemble member was run using the same radiative forcing for the historic (1920–2005) and future (2006–2100) but using a slightly different atmospheric state[62]. Simulations for the projected future climate in CESM-LENS are conducted for the Representative Concentration Pathway (RCP) 8.5. RCP 8.5 is the high emission scenario that considers an increase of 8.5 W/m^2 in radiative forcing by the end of the 21st century. Apart from precipitation and temperature, we obtained daily wind speed from CESM-LENS for the same period (1920–2100). CESM-LENS simulations are widely used for the assessment of drought and extreme climate events under the future climate[9,73,74]. To examine the role of greenhouse gages (GHG), industrial aerosols (AER), and land-use/land-cover (LULC) on extreme hot and dry events, we used simulations from the "Single Forcing" experiments of CESM-LENS[70]. The single-forcing experiment data from the CESM-LENS is available to address the individual roles of different forcings. The simulations were conducted using CESM1 with the same forcing, configuration, and initialization protocols as CESM-LENS but keeping the greenhouse gases, industrial aerosols, and LULC conditions fixed at 1920 while all other external anthropogenic and natural forcing factors follow historical and RCP 8.5 scenarios. The XGHG (no greenhouse gas, 1920–2080), XAER (no industrial aerosols, 1920–2080), and XLULC (no land-use/land-cover change, 1920–2029) have 20, 20, and 5 ensemble members, respectively.

Soil moisture simulations

As daily soil moisture simulations are not available from CESM-LENS, the Variable Infiltration Capacity (VIC) model[75,76] was used to simulate soil moisture using the observed and CESM-LENS forcing. The VIC model uses daily precipitation, maximum and minimum temperatures, and wind speed as meteorological inputs to simulate water budget. The VIC model (version: 4.2) was set up at 0.25° spatial resolution for entire India and run at full water balance mode at daily time-step. The VIC model simulates water and energy budget in each grid cell. Representation of sub-grid variability of vegetation and topography makes the VIC model distinct from the other land surface hydrological models. Vegetation parameters in the form of land use and land cover were obtained from NOAA-AVHRR[77] while soil parameters were derived using the Harmonic World Soil Database (HWSD). We used the calibrated soil parameters from Shah and Mishra (2016)[51] and Mishra et al. (2018)[17] for the VIC model. Six soil parameters were manually calibrated using the observed streamflow and performance of the VIC simulated soil moisture was evaluated against the in-situ and satellite-based soil moisture and evapotranspiration (ET)[51]. The VIC model estimates ET using Penman–Monteith method and has been used in the previous studies for estimating soil moisture based on flash droughts[25,78]. The meteorological forcing data were regridded to 0.25° using bilinear interpolation to conduct simulations using 40 ensemble members of CESM-LENS using the VIC model. Similarly, the VIC model simulations were conducted for XGHG, XAER, and XLULC scenarios for the 20, 20, and 5 ensemble members of CESM-LENS under the single-forcing experiment. To examine the influence of interpolation, we compared raw and regridded precipitation and temperatures. All-India averaged precipitation and temperature from the raw (at 1°), and regridded forcing at 0.25° was not found significantly different. A spin-up period of 20 years was used to make the VIC model simulations stable. The VIC simulated root-zone soil moisture (60cm[17]) was used for the identification of flash droughts and concurrent hot and dry extremes in India under the observed and projected future climate. Atmospheric variables (geopotential height, mean sea level pressure, integrated water vapor, and wind) were obtained from ERA-5 reanalysis to examine the drivers of the flash droughts.

Identification of flash droughts

Flash drought can be identified using precipitation, evapotranspiration, and soil moisture[21,22]. We used root-zone soil moisture simulated using the VIC model to identify flash droughts in India. We estimated mean soil moisture for each pentad (five-day period) in a calendar year. Therefore, 365/366 days were distributed in total of 73 pentads in a given year. The monsoon season (June–September) ranges from 30–55 pentad. After estimating the mean soil moisture for each pentad, percentile values were assigned for each pentad considering the climatology of 1951–2005 period. Empirical Weibull distribution was used to estimate soil moisture percentile (SMP[49]. Soil moisture below 20th percentile is considered a drought[18,49,79]. Flash drought can be identified based on the rapid onset[21], which means that soil moisture percentile can fall below a certain threshold in a quick time. If root-zone soil moisture declines from above 40th percentile to 20th (or less) percentile with an average rate of decline no less than five percentile in each pentad, the flash drought onset was identified[78]. If the declined soil moisture increases to 25th percentile, then the termination of the flash drought was considered. We considered flash droughts with a minimum duration of three pentads and a maximum duration of 18 pentads. The duration of each flash drought was estimated using the onset and termination. The maximum duration of 18 pentads was considered to avoid persistent long-term (conventional) droughts. Therefore, flash droughts that persisted longer and turned into drought were excluded from the analysis. More details of flash drought identification methodology are presented in supplementary Fig. 2.

DATA AVAILABILITY

Data used in this study are available from ERA-5 (https://cds.climate.copernicus.eu/cdsapp#!/dataset/reanalysis-era5-pressure-levels?tab=form) and CESM-LENS (https://www.cesm.ucar.edu/projects/community-projects/LENS/). All the data used in this study are available from the corresponding author upon reasonable request.

CODE AVAILABILITY

All the codes to estimate flash droughts in the observed and projected future climate can be obtained from the corresponding author.

Received: 18 August 2020; Accepted: 16 December 2020;
Published online: 14 January 2021

REFERENCES

1. Gadgil, S. & Gadgil, S. The Indian monsoon, GDP and agriculture. *Econ. Polit. Wkly.* **41**, 4887–4895 (2006).
2. Lobell, D. B., Sibley, A. & Ivan Ortiz-Monasterio, J. Extreme heat effects on wheat senescence in India. *Nat. Clim. Change* **2**, 186–189 (2012).
3. Ray, D. K., Gerber, J. S., Macdonald, G. K. & West, P. C. Climate variation explains a third of global crop yield variability. *Nat. Commun.* **6**, 1–9 (2015).
4. Gupta, R. et al. *Wheat productivity in indo-gangetic plains of India during 2010: Terminal heat effects and mitigation strategies*. http://46.20.115.203/download/cis/94590.pdf (2010).
5. Lesk, C., Rowhani, P. & Ramankutty, N. Influence of extreme weather disasters on global crop production. *Nature* **529**, 84–87 (2016).
6. Singh, D. et al. Climate and the Global Famine of 1876–78. *J. Clim.* **31**, 9445–9467 (2018).
7. Mishra, V., Aadhar, S., Asoka, A., Pai, S. & Kumar, R. On the frequency of the 2015 monsoon season drought in the Indo-Gangetic Plain. *Geophys. Res. Lett.* **43**, 12,102–12,112 (2016).
8. Gupta, A. K., Tyagi, P. & Sehgal, V. K. Drought disaster challenges and mitigation in India: strategic appraisal. *Curr. Sci.* **100**, 1795–1806 (2011).
9. Mishra, V., Thirumalai, K., Singh, D. & Aadhar, S. Future exacerbation of hot and dry summer monsoon extremes in India. *npj Clim. Atmos. Sci.* **3**, 10 (2020).
10. Zhang, Q., Kong, D., Singh, V. P. & Shi, P. Response of vegetation to different time-scales drought across China: spatiotemporal patterns, causes and implications. *Glob. Planet. Change* **152**, 1–11 (2017).
11. Fasullo, J. & Webster, P. J. A hydrological definition of Indian Monsoon onset and withdrawal. *J. Clim.* **16**, 3200–3211 (2003).
12. Mishra, V., Smoliak, B. V., Lettenmaier, D. P. & Wallace, J. M. A prominent pattern of year-to-year variability in Indian Summer Monsoon Rainfall. *Proc. Natl Acad. Sci. USA* **109**, 7213–7217 (2012).
13. Roxy, M. K. et al. Drying of Indian subcontinent by rapid Indian Ocean warming and a weakening land-sea thermal gradient. *Nat. Commun.* **6**, 7423 (2015).

14. Krishna Kumar, K., Hoerling, M. & Rajagopalan, B. Advancing Indian monsoon rainfall predictions. *Geophys. Res. Lett.* **32**, 1–4 (2005).
15. Mishra, A. K. & Singh, V. P. A review of drought concepts. *J. Hydrol.* **391**, 202–216 (2010).
16. Mishra, V. Long-term (1870–2018) drought reconstruction in context of surface water security in India. *J. Hydrol.* **580**, 124228 (2020).
17. Mishra, V. et al. Reconstruction of droughts in India using multiple land surface models (1951-2015). *Hydrol. Earth Syst. Sci.* **2000**, 1–22 (2018).
18. Mishra, V. et al. Drought and famine in India, 1870-2016. *Geophys. Res. Lett.* https://doi.org/10.1029/2018GL081477 (2019).
19. Niranjan Kumar, K., Rajeevan, M., Pai, D. S., Srivastava, A. K. & Preethi, B. On the observed variability of monsoon droughts over India. *Weather Clim. Extrem.* **1**, 42–50 (2013).
20. Kumar, K. K., Rajagopalan, B., Hoerling, M., Bates, G. & Cane, M. Unraveling the mystery of Indian monsoon failure during El Nino. *Science* **314**, 115–119 (2006).
21. Mo, K. C. & Lettenmaier, D. P. Heat wave flash droughts in decline. *Geophys. Res. Lett.* **42**, 2823–2829 (2015).
22. Otkin, J. A. et al. Flash droughts: a review and assessment of the challenges imposed by rapid-onset droughts in the United States. *Bull. Am. Meteorol. Soc.* **99**, 911–919 (2018).
23. Mo, K. C. & Lettenmaier, D. P. Precipitation deficit flash droughts over the United States. *J. Hydrometeorol.* **17**, 1169–1184 (2016).
24. Ford, T. W. & Labosier, C. F. Meteorological conditions associated with the onset of flash drought in the Eastern United States. *Agric. Forest Meteorol.* **247**, 414–423 (2017).
25. Mahto, S. S. & Mishra, V. Dominance of summer monsoon flash droughts in India. *Environ. Res. Lett*. https://doi.org/10.1088/1748-9326/abaf1d (2020).
26. Yuan, X., Ma, Z., Pan, M. & Shi, C. Microwave remote sensing of short-term droughts during crop growing seasons. *Geophys. Res. Lett.* **42**, 4394–4401 (2015).
27. Otkin, J. A. et al. Assessing the evolution of soil moisture and vegetation conditions during the 2012 United States flash drought. *Agric. Forest Meteorol.* **218–219**, 230–242 (2016).
28. Otkin, J. A. et al. Assessing the evolution of soil moisture and vegetation conditions during a flash drought–flash recovery sequence over the South-Central United States. *J. Hydrometeorol.* **20**, 549–562 (2019).
29. Asoka, A., Gleeson, T., Wada, Y. & Mishra, V. Relative contribution of monsoon precipitation and pumping to changes in groundwater storage in India. *Nat. Geosci.* **10**, 109–117 (2017).
30. Rodell, M., Velicogna, I. & Famiglietti, J. S. Satellite-based estimates of groundwater depletion in India. *Nature* **460**, 999 (2009).
31. Nanditha, J. S. et al. A seven-fold rise in the probability of exceeding the observed hottest summer in India in a 2 °C warmer world. *Environ. Res. Lett*. https://doi.org/10.1088/1748-9326/ab7555 (2020).
32. Mishra, V., Mukherjee, S., Kumar, R. & Stone, D. A. Heat wave exposure in India in current, 1.5 °C, and 2.0 °C worlds. *Environ. Res. Lett*. https://doi.org/10.1088/1748-9326/aa9388 (2017).
33. Im, E. S., Pal, J. S. & Eltahir, E. A. B. Deadly heat waves projected in the densely populated agricultural regions of South Asia. *Sci. Adv*. https://doi.org/10.1126/sciadv.1603322 (2017).
34. Rohini, P., Rajeevan, M. & Mukhopadhay, P. Future projections of heat waves over India from CMIP5 models. *Clim. Dyn.* **53**, 975–988 (2019).
35. Mazdiyasni, O. et al. Increasing probability of mortality during Indian heat waves. *Sci. Adv.* **3**, 1–6 (2017).
36. Pendergrass, A. G. et al. Flash droughts present a new challenge for subseasonal-to-seasonal prediction. *Nat. Clim. Change* **10**, 191–199 (2020).
37. Wang, L., Yuan, X., Xie, Z., Wu, P. & Li, Y. Increasing flash droughts over China during the recent global warming hiatus. *Sci. Rep.* **6**, 1–8 (2016).
38. Trenberth, K. E. et al. Global warming and changes in drought. *Nat. Clim. Change* **4**, 17–22 (2014).
39. Dai, A. Increasing drought under global warming in observations and models. *Nat. Clim. Change* **3**, 52–58 (2013).
40. AghaKouchak, A., Cheng, L., Mazdiyasni, O. & Farahmand, A. Global warming and changes in risk of concurrent climate extremes: Insights from the 2014 California drought. *Geophys. Res. Lett.* **41**, 8847–8852 (2014).
41. Diffenbaugh, N. S., Swain, D. L. & Touma, D. Anthropogenic warming has increased drought risk in California. *Proc. Natl Acad. Sci. USA* **112**, 3931–3936 (2015).
42. Mazdiyasni, O. & AghaKouchak, A. Substantial increase in concurrent droughts and heatwaves in the United States. *Proc. Natl Acad. Sci. USA* **112**, 11484–11489 (2015).
43. Kumar, K. R. et al. Climate Change scenarios for 21st Century India.pdf. *Curr. Sci.* **90**, 334–346 (2006).
44. Mall, R. K., Singh, R., Gupta, A., Srinivasan, G. & Rathore, L. S. Impact of climate change on Indian agriculture: a review. *Clim. Change* **78**, 445–478 (2006).
45. Pai, D. S. et al. Development of a new high spatial resolution (0. 25° × 0. 25°) Long Period (1901-2010) daily gridded rainfall data set over India and its comparison with existing data sets over the region. *Mausam* **65**, 1–18 (2014).
46. Srivastava, A. K., Rajeevan, M. & Kshirsagar, S. R. Development of a high resolution daily gridded temperature data set (1969-2005) for the Indian region. *Atmos. Sci. Lett.* **10**, 249–254 (2009).
47. Sheffield, J., Wood, E. F. & Roderick, M. L. Little change in global drought over the past 60 years. *Nature* **491**, 435–438 (2012).
48. Hobbins, M. T., Dai, A., Roderick, M. L. & Farquhar, G. D. Revisiting the parameterization of potential evaporation as a driver of long-term water balance trends. *Geophys. Res. Lett.* **35**, L12403 (2008).
49. Andreadis, K. M. & Lettenmaier, D. P. Trends in 20th century drought over the continental United States. *Geophys. Res. Lett.* **33**, L10403 (2006).
50. Sheffield, J., Goteti, G., Wen, F. & Wood, E. F. A simulated soil moisture based drought analysis for the United States. *J. Geophys. Res. Atmos.* **109**, D24108 (2004).
51. Shah, H. L. & Mishra, V. Hydrologic changes in Indian sub-continental river basins (1901-2012). *J. Hydrometeorol*. https://doi.org/10.1175/JHM-D-15-0231.1 (2016).
52. Martens, B. et al. GLEAM v3: satellite-based land evaporation and root-zone soil moisture. *Geosci. Model Dev.* **10**, 1903–1925 (2017).
53. Goswami, B. N. & Xavier, P. K. ENSO control on the south Asian monsoon through the length of the rainy season. *Geophys. Res. Lett.* **32**, n/a-n/a (2005).
54. Asharaf, S., Dobler, A. & Ahrens, B. Soil moisture–precipitation feedback processes in the Indian summer monsoon season. *J. Hydrometeorol.* **13**, 1461–1474 (2012).
55. Krishnan, R., Kumar, V., Sugi, M. & Yoshimura, J. Internal feedbacks from monsoon–midlatitude interactions during droughts in the Indian summer monsoon. *J. Atmos. Sci.* **66**, 553–578 (2009).
56. Rajeevan, M., Gadgil, S. & Bhate, J. Active and break spells of the indian summer monsoon. *J. Earth Syst. Sci.* **119**, 229–247 (2010).
57. Ramarao, M. V. S., Sanjay, J. & Krishnan, R. Modulation of summer monsoon subseasonal surface air temperature over India by soil moisture-temperature coupling. *Mausam* **67**, 53–66 (2016).
58. Goswami, B. N., Ajayamohan, R. S., Xavier, P. K. & Sengupta, D. Clustering of synoptic activity by Indian summer monsoon intraseasonal oscillations. *Geophys. Res. Lett.* **30**(8), 1431 (2003).
59. Gadgil, S. The Indian monsoon and its variability. *Annu. Rev. Earth Planet. Sci.* **31**, 429–467 (2003).
60. Goswami, B. N., Mohan, R. S. A., Goswami, B. N. & Mohan, R. S. A. Intraseasonal oscillations and interannual variability of the Indian summer monsoon. *J. Clim.* https://doi.org/10.1175/1520-0442 (2001).
61. Krishnamurthy, V. & Shukla, J. Intraseasonal and seasonally persisting patterns of Indian monsoon rainfall. *J. Clim.* **20**, 3–20 (2007).
62. Kay, J. E. et al. The Community Earth System Model (CESM) Large Ensemble Project: a community resource for studying climate change in the presence of internal climate variability. *Bull. Am. Meteorol. Soc.* **96**, 1333–1349 (2015).
63. Ashfaq, M., Rastogi, D., Mei, R., Touma, D. & Leung, L. R. Sources of errors in the simulation of south Asian summer monsoon in the CMIP5 GCMs. *Clim. Dyn.* **49**, 193–223 (2017).
64. Menon, A., Levermann, A., Schewe, J., Lehmann, J. & Frieler, K. Consistent increase in Indian monsoon rainfall and its variability across CMIP-5 models. *Earth Syst. Dyn.* **4**, 287–300 (2013).
65. Bretherton, C. S., Smith, C. & Wallace, J. M. An intercomparison of methods for finding coupled patterns in climate data. *J. Clim.* **5**, 541–560 (1992).
66. Lorenz, R., Jaeger, E. B. & Seneviratne, S. I. Persistence of heat waves and its link to soil moisture memory. *Geophys. Res. Lett.* **37**, L09703 (2010).
67. Miralles, D. G., Teuling, A. J., Van Heerwaarden, C. C. & De Arellano, J. V. G. Mega-heatwave temperatures due to combined soil desiccation and atmospheric heat accumulation. *Nat. Geosci.* **7**, 345–349 (2014).
68. Rustamji, K. F. The terrible drought of 1979. *India Int. Cent. Q.* **6**, 317–328 (1979).
69. Chaturvedi, R. K., Joshi, J., Jayaraman, M. & Bala, G. Multi-model climate change projections for India under representative concentration pathways. *Curr. Sci.* **103**, 791–802 (2012).
70. Deser, C. et al. Insights from Earth system model initial-condition large ensembles and future prospects. *Nat. Clim. Change* **10**, 277–286 (2020).
71. Shah, D. & Mishra, V. Integrated Drought Index (IDI) for drought monitoring and assessment in India. *Water Resour. Res.* **55**, 9191–9210 (2019).
72. Maurer, E. P., Wood, A. W., Adam, J. C., Lettenmaier, D. P. & Nijssen, B. A long-term hydrologically-based data set of land surface fluxes and states for the conterminous {United States}. *J. Clim.* **15**, 3237–3251 (2002).
73. Ault, T. R. On the essentials of drought in a changing climate. *Science* **368**, 256–260 (2020).
74. Aadhar, S. & Mishra, V. Increased drought risk in South Asia under warming climate: Implications of uncertainty in potential evapotranspiration estimates. *J. Hydrometeorol*. https://doi.org/10.1175/jhm-d-19-0224.1 (2020).

75. Liang, X., Wood, E. F. & Lettenmaier, D. P. Surface soil moisture parameterization of the VIC-2L model: evaluation and modification. *Glob. Planet. Change* **13**, 195–206 (1996).
76. Cherkauer, K. A., Bowling, L. C. & Lettenmaier, D. P. Variable infiltration capacity cold land process model updates. *Glob. Planet. Change* **38**, 151–159 (2003).
77. Hansen, M. C., Defries, R., Townshend, J. R. G. & Sohlberg, R. Global land cover classification at 1 km spatial resolution using a classification tree approach. *Int. J. Remote Sens.* **21**, 1331–1364 (2000).
78. Yuan, X. et al. Anthropogenic shift towards higher risk of flash drought over China. *Nat. Commun*. https://doi.org/10.1038/s41467-019-12692-7 (2019).
79. Svoboda, M. et al. The drought monitor. *Bull. Am. Meteorol. Soc.* **83**, 1181–1190 (2002).

ACKNOWLEDGEMENTS

We acknowledge the financial assistance from the Ministry of Earth Science. The data availability from NCAR-CESM, ERA-5, and India Meteorological Department is greatly appreciated.

AUTHOR CONTRIBUTIONS

V.M. designed the study, conducted the analysis, and wrote the manuscript. S.A. processed CESM-LENS data and ran the VIC model simulations. S.S.M. helped in processing ERA-5 dataset.

COMPETING INTERESTS

The authors declare no competing interests.

ADDITIONAL INFORMATION

Supplementary information is available for this paper at https://doi.org/10.1038/s41612-020-00158-3.

Correspondence and requests for materials should be addressed to V.M.

Reprints and permission information is available at http://www.nature.com/reprints

Publisher's note Springer Nature remains neutral with regard to jurisdictional claims in published maps and institutional affiliations.